

Vacuumed collagen-impregnated bioglass scaffolds: Characterization and influence on proliferation and differentiation of bone marrow stromal cells

Hueliton Wilian Kido ¹, Paulo Roberto Gabbai-Armelin,¹ Ingrid Regina Avanzi,¹ Antonio Carlos da Silva,² Kelly Rossetti Fernandes,¹ Carlos Alberto Fortulan,³ Ana Claudia Muniz Rennó¹

¹Department of Biosciences, Federal University of São Paulo (UNIFESP), Santos, SP, Brazil

²Nuclear and Energy Research Institute (IPEN), São Paulo, SP, Brazil

³Department of Mechanical Engineering, University of São Paulo (USP) São Carlos, SP, Brazil

Received 14 September 2017; revised 9 February 2018; accepted 6 March 2018

Published online 23 March 2018 in Wiley Online Library (wileyonlinelibrary.com). DOI: 10.1002/jbm.b.34112

Abstract: This study evaluated physical–chemical characteristics of a vacuumed collagen-impregnated bioglass (BG) scaffolds and bone marrow stromal cells (BMSCs) behavior on those composites. scanning electron microscope and energy dispersive x-ray spectroscopy demonstrated collagen (Col) was successfully introduced into BG. Vacuum impregnation system has showed efficiency for Col impregnation in BG scaffolds (approximately 20 wt %). Furthermore, mass weight decreasing and more stabilized pH were observed over time for BG/Col upon incubation in phosphate buffered saline compared to plain BG under same conditions. Calcium evaluation (Ca assay) demonstrated higher calcium uptake for BG/Col samples compared to BG. In addition, BG samples presented hydroxyapatite crystals formation on its surface after 14 days in simulated body fluid solution, and signs of initial degradation were observed for BG and BG/Col after 21 days. Fourier transform infrared spectroscopy spectra for both

groups indicated peaks for hydroxyapatite formation. Finally, a significant increase of BMSCs viability for both composites was observed compared to control group, but no increase of osteogenic differentiation-related gene expressions were found. In summary, BG/Col scaffolds have improved degradation, pH equilibrium and Ca mineralization over time, accompanied by hydroxyapatite formation. Moreover, both BG and BG/Col scaffolds were biocompatible and noncytotoxic, promoting a higher cell viability compared to control. Future investigations should focus on additional molecular and *in vivo* studies in order to evaluate biomaterial performance for bone tissue engineering applications. © 2018 Wiley Periodicals, Inc. *J Biomed Mater Res Part B: Appl Biomater* 107B: 211–222, 2019.

Key Words: vacuum impregnation system, bioglass, collagen, scaffold, bone marrow stromal cells

How to cite this article: Kido HW, Gabbai-Armelin PR, Avanzi IR, Silva AC, Fernandes KR, Fortulan CA, Rennó ACM 2019. Vacuumed collagen-impregnated bioglass scaffolds: Characterization and influence on proliferation and differentiation of bone marrow stromal cells. *J Biomed Mater Res Part B* 2019;107B:211–222.

INTRODUCTION

Nowadays many materials have been developed with the aim of stimulating bone metabolism and accelerating the process of bone healing. In addition, the use of composite materials for bone tissue engineering is of great interest due to the combination of different biological properties, resulting in a bone graft with improved osteogenic properties.¹ Especially, the association of an inorganic filler with an organic one can mimic bone tissue and constitute a more adequate bone graft.¹

One of the most promising inorganic materials for bone regenerative therapies is the Bioglass 45S5 (BG), which presents excellent osteogenic properties and high levels of bioactivity.^{2–4} BG is a synthetic silica-based bioactive material, able to bond bone tissue, forming a silica gel layer,

which attracts bone cells and increase deposition of newly bone tissue.² Similarly, collagen (Col) is a common matrix used for bone grafts, especially combined with other materials.⁵ Col is the most abundant protein of human body and a predominant extracellular matrix (ECM) component.⁶ It is biocompatible, has a high affinity to water, controllable biodegradation, hemostatic properties, low inflammatory host response, being a very useful material in biomedical applications.^{5,7,8}

In this context, Col and BG composite scaffolds resembling the organic and inorganic bone ECM composition have been extensively investigated for bone tissue engineering purposes.^{9,10} Many authors demonstrated an increased biological performance of BG/Col composites on the acceleration of bone formation and restoration.^{9–11} An ectopic

Additional Supporting Information may be found in the online version of this article.

Correspondence to: H. W. Kido; e-mail: kidohw@gmail.com

Contract grant sponsor: Fundação de Amparo à Pesquisa do Estado de São Paulo (FAPESP); contract grant number: 2014/23471-1 (to H.W.K.)

in vivo mineralization was observed in the subcutaneous tissue of rats when was applicated an injectable BG/Col composite, determining its osteoinductive properties and potential to be a novel therapeutic approach for bone tissue engineering.¹² However, BG/Col osteoconductive properties may not be sufficient to achieve complete defect filling under critical conditions, like poorly vascularized sites and (elderly) patients with metabolic disorders. Consequently, osteopromotive or osteoinductive factors introduction to BG/Col is necessary to improve their biological performance.

Toward this goals, biomaterials and cell therapy [mainly bone marrow stromal cells [BMSCs]] present synergistic combination to optimally yield functional bone tissue for implantation purposes.^{13–15} Different cell types have been used for bone tissue engineering from primary adult osteoblasts (bone cells) to BMSCs in different animal models.^{13,15,16} Despite a few positive results, findings are still controversial and there is poor predictive capacity for clinical applications from the animal models.^{17,18}

Based on the need of more effective treatments for bone tissue engineering, it was hypothesized that the addition of BMSCs to BG/Col scaffolds would offer a novel way of improving material performance. Introduction of BMSCs was designed to integrate high bioactivity to the scaffold, increasing material osteogenic potential. Despite these possible advantages, there is still limited understanding of interactions between BG and BG/Col materials and the cellular component phases. Moreover, most of methods for Col impregnation into BG is based on immersion of the bioactive material in solutions containing Col,^{19,20} which are not enough for an efficient impregnation using this organic component. In this context, improved and innovative methods for Col impregnation should be developed to guarantee a homogeneous distribution of this component into the glass and, consequently, an optimized treatment. Following this line, we hypothesized that the novel vacuum system would be more effective for impregnating BG scaffolds with Col compared to Col immersion bath. Thus, the aims of the present study were (i) to verify the efficiency of a novel system for obtaining vacuumed Col-impregnated BG scaffolds, (ii) to determine physical–chemical properties of the scaffolds, and (iii) to investigate BMSCs cell behavior seeded into the construction by evaluating cell viability and temporal expression pattern of osteogenic genes using quantitative real-time polymerase chain reaction (qRT-PCR).

MATERIALS AND METHODS

Materials

BG ($\text{SiO}_2\text{-CaO-Na}_2\text{O-P}_2\text{O}_5$) was provided by Materials Science and Technology Center from Institute of Energy and Nuclear Research (particle size: 125–250 μm ; IPEN, Brazil). Commercially available fibers of bovine tendon collagen type I (Col) used in the present study was purchased from United States Biological Life Sciences company (US Biological Life Sciences).

Synthesis of the BG scaffolds

BG scaffolds were manufactured using 100 mL of a suspension containing 67 vol % of isopropyl alcohol (Sigma-Aldrich, São Paulo, Brazil), 3 vol % of polyvinyl butiral (Butvar B-98), 24 vol % of naphthalene (used as porogenic agent with two different sizes of 177–300 and 300–600 μm (1:1); Sigma-Aldrich) and 6 vol % of BG. After mixing isopropyl alcohol, polyvinyl butyral, and BG powder for 1 h, naphthalene was added and homogenized and set to dry at RT. The resulting granulated powder was passed in a nylon sieve (18 MESH—1 mm), and pressed in two steps. In the first step, the powder (0.07 g per scaffold) was uniaxially pressed in a cylindrical stainless-steel mold (8 mm in diameter) at 20 MPa for 15 s. Then, in the second step, the samples were isostatically pressed at 100 MPa for 30 s. Afterward, the following heating rates were used in the sintering process: room temperature to 120°C (1°C/min), 120 to 600°C (2°C/min), 600 to 900°C (5, 6°C/min), holding at maximum temperature (900°C) for 1 h, followed by cooling to room temperature inside the furnace.^{21,22} Finally, BG scaffolds with approximately 8 mm diameter and 2 mm thickness were obtained.

Col impregnation of the BG scaffolds

For manufacturing of Col-impregnated BG scaffolds, an adapted protocol from Camilo et al.²¹ was used. Differently from Camilo, which used this method for coating of alumina with bioactive ceramics,²¹ in present work this technique was utilized for Col effective impregnation into porous BG scaffolds. Briefly, 0.5 g of Col fibers were dissolved in 100 mL of acetic acid (pH 2.5) for 24 h at 4°C.^{5,23} Col solution was homogenized with a mixer and stored at 4°C for further use. BG scaffolds ($n = 50$) and Col solution (15 mL) were put inside a recipient (placed in vacuum Erlenmeyer flask) which had subparts separated by sieve [Figure 1(A)]. By using the vacuum (10^{-3} Torr), air molecules were removed of the system through vent holes. Afterward, this compartment was inverted, vacuum was turned off, and Col solution was put in contact to BG scaffolds for 1 min, in order to proceed with the impregnation of the scaffolds [Figure 1(B)]. For comparison purposes, Col-impregnated BG scaffolds were also obtained after soaking BG scaffolds in an Col solution without using the vacuum system, following the methodology described previously.^{19,20}

After Col impregnation process, samples were taken out of the solution and dried for 24 h on metal support which had under it silica gel. Then, samples were neutralized inside desiccator with 5 mL of ammonium hydroxide (Sigma-Aldrich) vapor for 24 h.²⁴

All samples (BG and BG/Col scaffolds) were sterilized with ethylene oxide before analyzes. Inorganic and organic components proportion (wt %) of the BG/Col-based scaffolds (using vacuum system or immersion bath) was verified by weight difference (g) between BG/Col and BG (i.e., BG scaffold weight after and before impregnation with Col; $n = 7$).

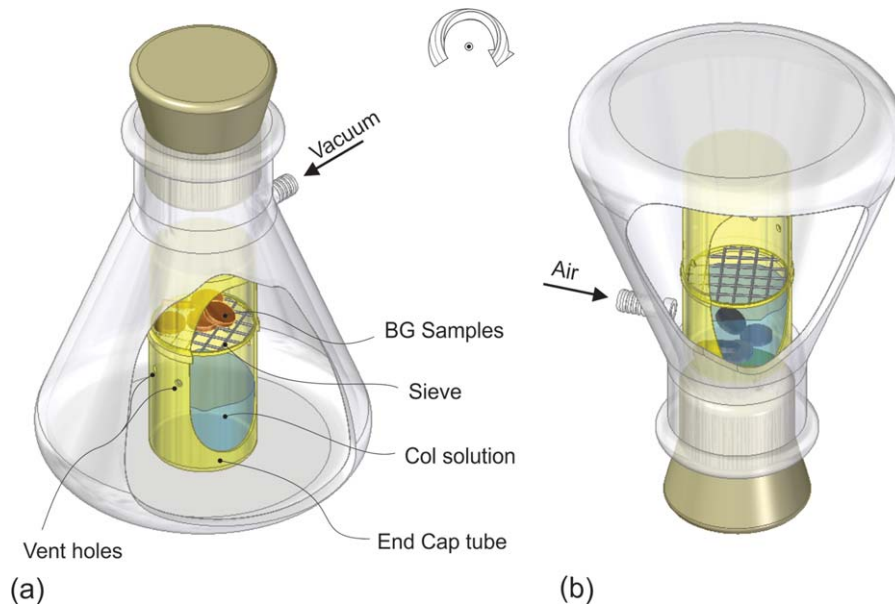


FIGURE 1. Schematic representation of the vacuum collagen impregnation process. BG samples and Col solution under vacuum impregnation system (A); BG samples in contact to Col solution after turning off the vacuum and inverting the impregnation system (B).

Characterization of the BG/Col scaffolds

Scanning electron microscope. Materials morphology was first examined by scanning electron microscope (SEM) observation (Jeol 6310). BG and BG/Col scaffolds (using vacuum system or immersion bath for Col impregnation) were mounted on aluminum stubs using carbon tape and sputter-coated with gold/palladium prior to examination. SEM images of the BG and BG/Col scaffolds with the magnification of $\times 85$ and $\times 500$ were obtained.

Porosity and pores sizes measurements. Apparent porosity (P) was obtained by immersion density test, using a method based in Archimedes' principle, as described previously.²¹ For this purpose, weight scale (Mettler Toledo, AB 204) and a Becker support apparatus with tray were used. Briefly, samples of BG scaffolds ($n = 5$) were weighted for obtaining their dry weight (Dw). Subsequently, these samples were immersed in ethanol for 24 h for measuring the immersed weight (Iw) and wet weight (Ww). P was obtained by using the following equation:

$$P = [(Ww - Dw)/(Ww - Iw)] \times 100 \quad (1)$$

Additionally, pores sizes of BG scaffolds were evaluated utilizing SEM micrographs with an image analysis software (ImageJ, 1.51p) following methodology described previously.²²

Energy dispersive X-ray spectroscopy. Distribution map of elements present on surface of the materials were obtained using SEM (ultrahigh-resolution SEM; FEI Sirion) equipped with OIM Pegasus energy dispersive x-ray spectroscopy (EDX, Edax). For this analysis, the following parameters were used: standard Co for calibration, electron beam of 20 kV, focal length of 25 mm, dead time of 30%, current of 2.82 A and I probe of 2.5 nA.

Mass loss quantification and pH measurements (in phosphate buffered saline).

For the mass loss and pH evaluations, BG and BG/Col scaffolds were weighed, immersed in 3 mL of phosphate buffered saline (PBS) (10 mM, pH 7.4) and incubated at 37°C. BG and BG/Col samples ($n = 5$ per period) were analyzed after 1, 3, 7, 14, and 21 days of immersion. According to each experimental period, samples were removed from the medium and vacuum-dried overnight before measuring the mass. Then, samples were weighed and the percentage of mass loss was calculated by the difference between the initial and final value of the weight of the samples. Directly after removal of the materials, the pH of the PBS medium was measured (Quimis, São Paulo, Brazil).

Calcium assay. For the calcium deposition study, BG and BG/Col samples were placed in 7.5 mL of conventional simulated body fluid (SBF) according to Kokubo and Takadama.²⁵ After 1, 3, 7, 14, and 21 days of immersion, solutions in contact with BG and BG/Col samples were saved for analysis of calcium content using the orthocresolphthalein complexone assay (Sigma Chemical, St. Louis, MO), as described previously.^{26,27} These solutions were incubated overnight in 1 mL 0.5N acetic acid on a shaker table. After the incubation period, 300 mL working reagent was added to 10 mL sample or standard in a 96-well plate. Afterward, plate was incubated for 10 min at room temperature. Absorbance of each well was measured on a microplate spectrophotometer at 570 nm (Bio-Tech Instruments, Winooski, VT). A standard curve was generated by serial dilutions of $CaCl_2$ stock (range 0–100 mg/mL). Data were acquired from quadruplicate samples and measured in duplo. The Ca depletion was cumulatively plotted by measuring the difference between the SBF solution in the

TABLE I. Primers and the Expected PCR Product Size at Indicated Annealing Temperatures for Each Gene Analyzed

Gene	Forward	Reverse Primer	Annealing Temperature (°C)
bActina ^a	ACCAGTTCGCCATGGATGAC	TGCCGGATGGATGAC	60
ALP	G AACTACATCCCCACGTCATG	CCCAGGCACAGTGGTCAAG	60
Runx2	TTATGTGTGCCTCCAACCTGTGT	GGTTTCTTTCCCCTCAATTTGT	60

^abActina, beta-Actin; ALP, alkaline phosphatase; and Runx2, runt-related transcription factor 2.

presence of BG and BG/Col samples and the Ca concentration in the sample-free SBF solutions.

Morphology after SBF incubation. Morphology postincubation was analyzed by SEM (Jeol 6310) after 1, 14, and 21 days of SBF incubation for checking signs of degradation and hydroxyapatite (HA) formation.

Fourier transform infrared spectroscopy. Fourier transform infrared spectroscopy (FTIR) analysis (Perkin-Elmer 1700, UK) were used at day 14 of SBF incubation for evaluating the presence of HA characteristics peaks. Analyses were performed in the range of 400–4000 cm⁻¹ with resolution of 2 cm⁻¹. The samples, in powder form, were scanned 100 times for each FTIR measurement and the spectrum obtained was the scans average.

Cell culture. BMSC were obtained from the tibia and femur of Wistar rats (10–12 weeks), according to a previous protocol.²⁸ Briefly, BMSCs were isolated from male rats by flushing the marrow with culture medium (minimum essential medium eagle alpha modification: α -MEM, supplemented with 10% fetal bovine serum and 1% antibiotic; Vitrocell, Campinas, Brazil) into a 50 mL tube with an inserted needle into one open end of the bone. Isolated BMSCs adhered to plastic surface and were easily expanded²⁸ in growth medium (α -MEM) using a 75 cm² cell culture flask. Flask was placed in an incubator with a temperature of 37°C, a humidified environment and containing 5% CO₂, with medium changed every 2 days. Cells were maintained at subconfluent densities and cultivated every 2–3 days until their use.

Cell viability. For this analysis, cells were then transferred to 24-well plates (50,000 cell for cm²) and cultured in the incubator (37°C and 5% CO₂) in direct contact to BG and BG/Col scaffolds ($n = 3$ per group for each period) with osteoinductive

medium (growth medium with 1% β -Glycerophosphate, 1% 2-phospho-L-ascorbic acid trisodium salt and 0.1% dexamethasone) during 3, 7, 14, and 21 days. This medium was refreshed twice a week. Control group (CG, $n = 3$) consisted of wells filled with BMSCs and osteoinductive medium.

After each experimental period, wells were rinsed with PBS to remove unattached cells and wash out the remaining serum, and a 10% alamarBlue[®] solution (Thermo Fisher Scientific, São Paulo, Brazil) (500 μ L) was then added into each well of 24-well plates which were incubated in dark for 3 h. After, 200 μ L of solution (in duplicate) were aliquoted into wells of a 96-well plate to be measured by a spectrophotometric plate reader at 570 and 600 nm. From the values obtained, the calculation for proliferation could be obtained by the percentage reduction of alamarBlue according to manufacturer's instructions.

Quantitative RT-PCR. BG and BG/Col scaffolds effects on the BMSC differentiation were assessed from expression levels of osteogenic-related genes (alkaline phosphatase [ALP]; Runt related transcription factors 2 [Runx2]) (Table I) using qRT-PCR. BMSCs were cultured in 24-well (10,000 cells/cm²) plates for 7 and 14 days in contact with BG and BG/Col scaffolds (1 scaffold/well; $n = 3$). Then, after each experimental period, total ribonucleic acid (RNA) was isolated using a RNA Isolation Kit (RNeasy Mini Kit, QIAGEN, São Paulo, Brazil). Potential deoxyribo nucleic acid (DNA) contamination was removed by RNase-free DNase I (Thermo Fisher Scientific). Complementary DNA (cDNA) was generated from the RNA using the high-capacity cDNA reverse transcription kit (Thermo Fisher Scientific). The qRT-PCR analysis was performed on thermal cycler (7500 Fast Real-Time PCR System, Applied Biosystems, Waltham) using SYBR Green detection reagent (Thermo Fisher Scientific). Gene relative expression was normalized against the

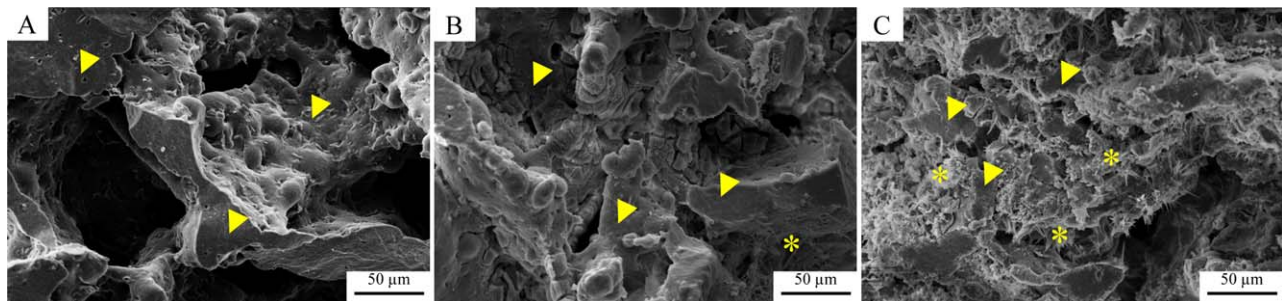


FIGURE 2. SEM images of BG (A) and BG/Col impregnated by immersion bath (B) and vacuum system (C). Arrow heads represent BG and asterisks represent Col layer. Magnifications of $\times 500$.

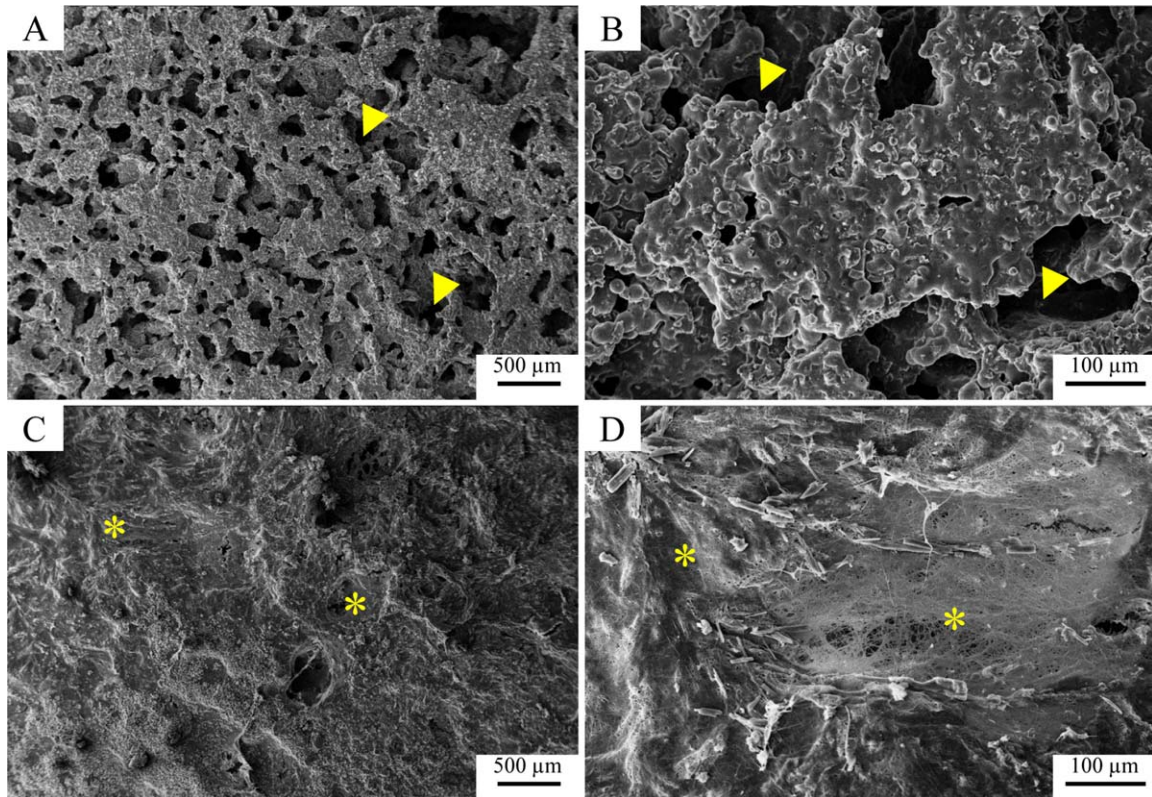


FIGURE 3. SEM images of the BG (A,B) and BG/Col (C,D) scaffolds at magnifications of $\times 85$ (A,C) and $\times 500$ (B,D). Arrow heads represent pores in the materials and asterisks represent collagen layer.

housekeeping gene beta-Actin (bActin). Relative expression was calculated using the following formula: $2^{-\Delta\Delta CT}^{29}$

Statistical analysis

Data were expressed as mean \pm standard deviation. Statistical analyses were done using GraphPad Prism 6 (GraphPad Software, San Diego, CA). Shapiro-Wilk normality test was utilized to check distribution. Kruskal-Wallis test and Dunn *post hoc* were used for nonparametric data. One-way

analysis of variance and Tukey multiple comparisons post-tests were used for parametric data. Differences were significant at $p \leq 0.05$.

RESULTS

Synthesis of the scaffolds

Porous BG scaffolds were successfully obtained using naphthalene (porogenic agent) and isostatic pressure to aggregate BG powder. These scaffolds were cohesive and easy to

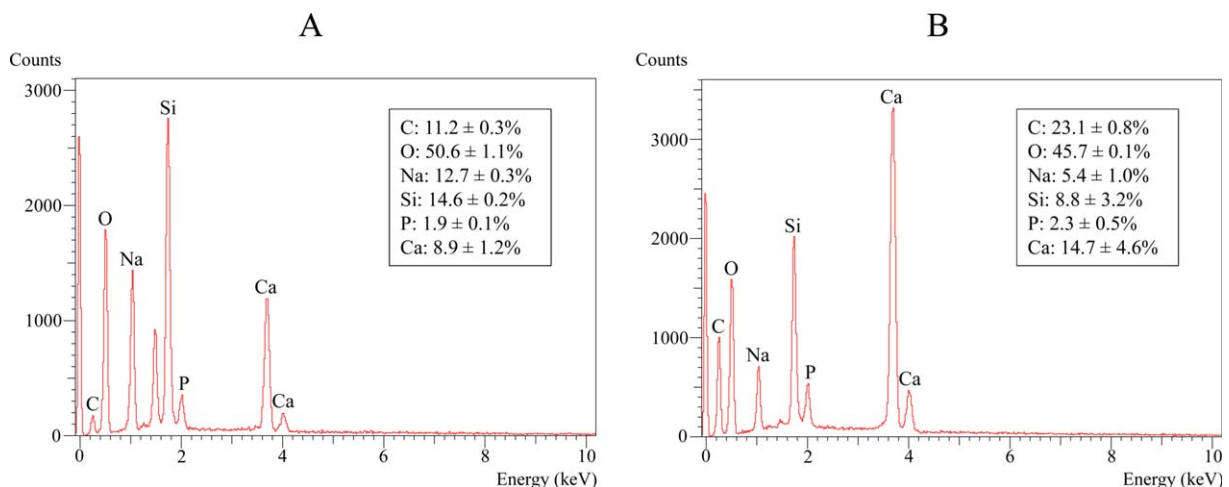


FIGURE 4. EDX analysis performed on BG (A) and BG/Col (B). The % of each element on the materials are depicted in the box. C, carbon; O, oxygen; Na, sodium; Si, silicon; P, phosphor; and Ca, calcium.

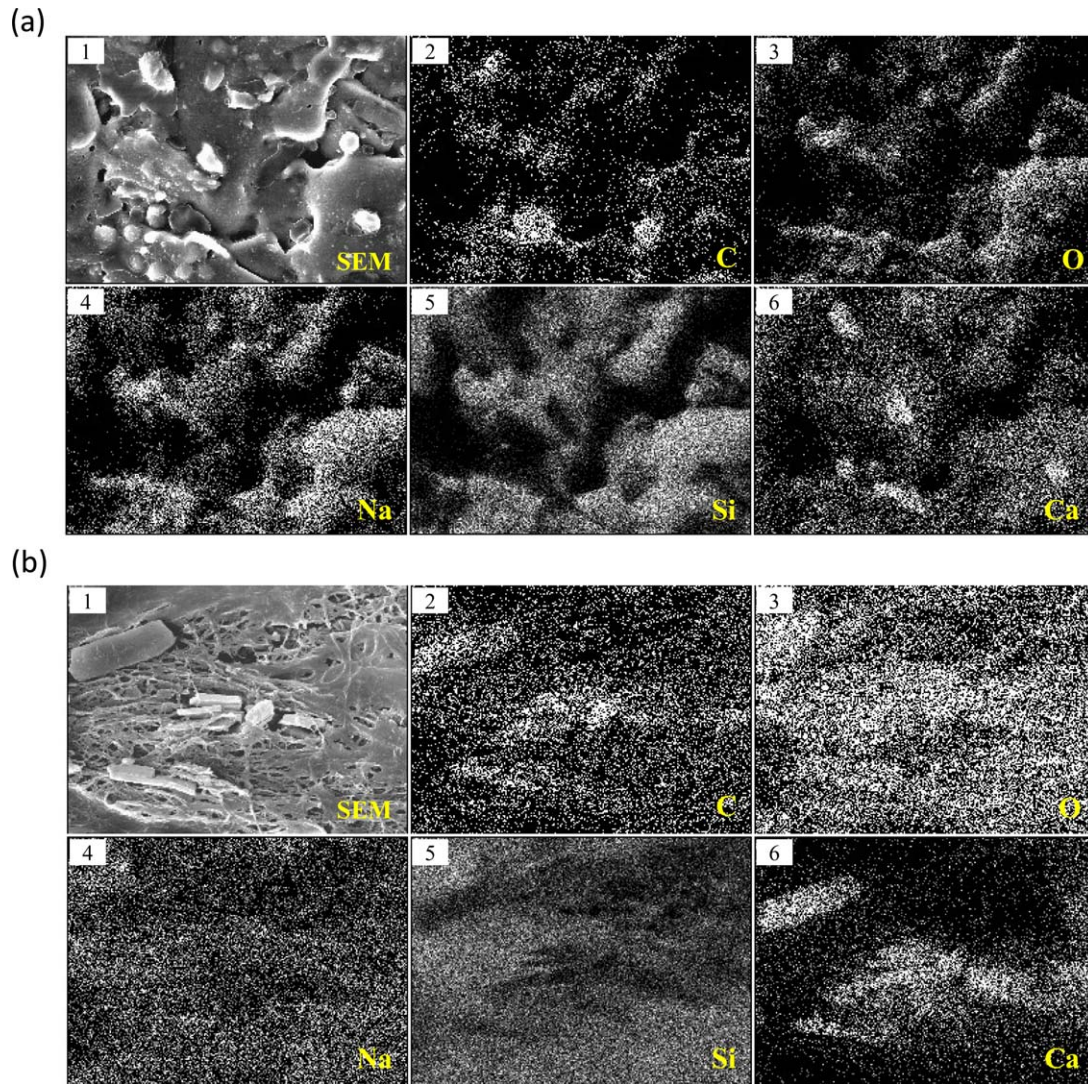


FIGURE 5. EDX mapping of the chemical elements on BG (A) and BG/Col (B) samples. SEM images of the selected points for EDX analysis [(A)1,(B)1]. EDX mapping for C [(A)2,(B)2]; for O [(A)3,(B)3]; for Na [(A)4,(B)4]; for Si [(A)5,(B)5] and for Ca [(A)6,(B)6].

handle. Vacuum system for impregnating collagen into scaffolds made it effectively feasible to produced BG-impregnated scaffolds, since a more evident presence of collagen was observed inside BG/Col obtained with vacuum system [Figure 2(C)] compared to the immersion one [Figure 2(B)]. Interestingly, the resulting proportion of BG/Col using vacuum system and immersion bath was approximately 80/20 and 98/02 wt %, respectively.

Characterization of the BG/Col scaffolds

SEM. SEM images showed a homogeneous pores distribution on the surface of BG scaffolds [Figure 3(A,B)]. For BG/Col samples, a smoother surface could be observed related to the Col fibers which was covering the of the scaffolds [Figure 3(C,D)].

Porosity and pores sizes measurements. By immersion density test, BG scaffolds resulted in $77.08 \pm 2.27\%$ of porosity. The pores were interconnected with sizes of $234.24 \pm 185 \mu\text{m}$.

EDX—Elements concentration. Figure 4 presents concentration (%) of the chemical elements for BG and BG/Col samples assessed by the EDX. Main elements found in both groups were C, O, Na, Si, P, and Ca [Figure 4(A,B)]. Interestingly, BG/Col showed increased percentage of C ($\sim 23\%$) and Ca ($\sim 15\%$), and diminished percentage of O ($\sim 46\%$), Na ($\sim 5\%$) and Si ($\sim 9\%$) when compared to BG (C $\sim 11\%$; Ca $\sim 9\%$; O $\sim 51\%$; Na $\sim 13\%$; Si $\sim 15\%$).

EDX—Map of elements. Figure 5 represents EDX compositional map of the chemical elements on the BG and BG samples. By this analysis, mappings and distributions of elements C, O, Na, Si and Ca on the surface of the materials could be verified. Curiously, mapping and distribution for each element were well-defined for BG [Figure 5(A)], and, contrasting that, EDX mapping for BG/Col indicated homogeneous distribution of elements on materials surface [Figure 5(B)].

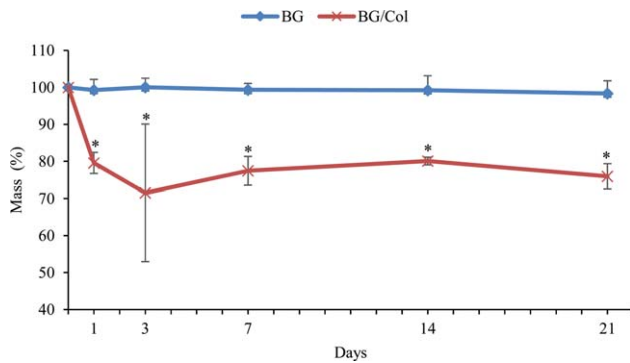


FIGURE 6. Mass measurements for BG and BG/Col samples upon incubation in PBS. * BG/Col compared to BG; $0.015 < p < 0.029$.

Mass measurements. It was observed in Figure 6 that BG samples did not present any mass variation in evaluated periods, maintaining similar weight from day 1 to the end of the experiment (21 days). Contrary to this behavior, BG/Col samples presented mass loss, in the first experimental period (1 day), compared to their initial mass, reaching 79.6%. The mass loss continued for BG/Col up to 72% for up to 3, after which a plateau was reached until the last time point (21 days). In all periods, BG/Col samples presented statistically different values of mass loss when compared to BG samples ($0.015 < p < 0.029$).

pH measurements. Figure 7 presents pH behavior of the medium (PBS) for BG and BG/Col scaffolds during the experimental periods. For BG samples, an increase of pH in day 1 was observed (pH 10) compared to the initial pH of the PBS (pH 7.4). At day 3, pH increasing continued, reaching the value of 11 and remaining stable until the last evaluated period (21 days). BG/Col samples showed a slight pH increase after 1 day of incubation (pH 8). Still, after three days of incubation, it was verified that BG/Col samples presented pH close to 9, which was maintained in the other periods. For BG/Col samples, a statistically lower pH value was observed when compared to BG samples in all evaluated periods ($0.015 < p < 0.029$).

Ca assay. Figure 8 demonstrated Ca concentration in SBF solution after immersion of BG and BG/Col samples for up to 21 days. For BG samples, a continuous Ca release was observed from day 1 to 7, reaching 381.64 μg . After 7 days of BG incubation, it was verified that the samples started a Ca uptake process, resulting in values of 123.27 and 301.28 μg at days 14 and 21, respectively. BG/Col samples showed slight calcium release in the first experimental point (138.52 μg), followed by an uptake of this ion at days 3, 7, and 14, resulting in values of 23.38, 397.30 and 607.03 μg , respectively. At day 21, Ca release was observed, reaching 428.10 μg . Statistically lower values for Ca were observed for BG/Col compared to BG at days 7 and 14 ($p < 0.0001$).

Morphology after incubation. SEM analysis demonstrated that HA formation could be observed on the surface of BG

scaffolds at days 14 and 21 of SBF incubation (Figure 9). On the other hand, no characteristic globular crystals for HA were observed on the surface of BG/Col-based materials (Figure 9). For both materials, signs of degradation were noticed after 21 days of incubation. These signs were most of them like crackings on the surface and fibers ruptures for BG and BG/Col, respectively (Figure 9).

FTIR. Figure 10 presents BG powder (base) FTIR spectra for BG powder with no incubation, and BG and BG/Col scaffolds after 14 days of SBF immersion. For BG powder, no evident peaks associated to P-O ($500\text{--}600\text{ cm}^{-1}$) were noticed. Differently of that, defined peaks to P-O (crystalline and vitreous) were observed for BG and BG/Col scaffolds around $500\text{--}600\text{ cm}^{-1}$.

Cell viability. Figure 11 shows results of the cell viability assay. In general, BG and BG/Col presented a tendency in increasing cell viability compared to CG overtime. After 3 days of culture, significant differences were observed comparing BG to CG ($p < 0.01$) and BG/Col ($p < 0.001$). At day 7 and 14, statistically higher values for viability was found for both BG and BG/Col when compared to CG ($p < 0.05$). Also, at these same periods, BG presented significant higher values compared to BG/Col ($p < 0.01$). Interestingly, no statistical difference was observed at day 21 comparing BG to BG/Col ($p > 0.05$) and both groups showed significant higher cell viability compared to CG ($p < 0.001$).

qRT-PCR evaluation. Figure 12 demonstrates gene expression of ALP and Runx2 for CG, BG and BG/Col groups after 7 and 14 days of incubation with BMSCs. BG group showed statistically significant higher value for ALP expression only at day 7 when compared to BG/Col ($p < 0.05$) [Figure 12(A)]. No other significant difference for ALP gene expression was verified among other groups ($p > 0.05$). No statistical difference was observed for Runx2 gene expression among all groups during evaluated periods [Figure 12(B)].

DISCUSSION

This study aimed to evaluate physical-chemical characteristics of a BG/Col scaffold and *in vitro* BMSCs behavior in contact with composites (by means of cell viability and gene

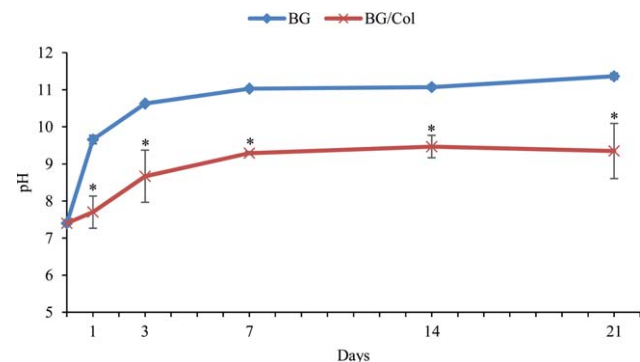


FIGURE 7. pH behavior of the incubation medium for BG and BG/Col scaffolds. * BG/Col compared to BG; $0.015 < p < 0.029$.

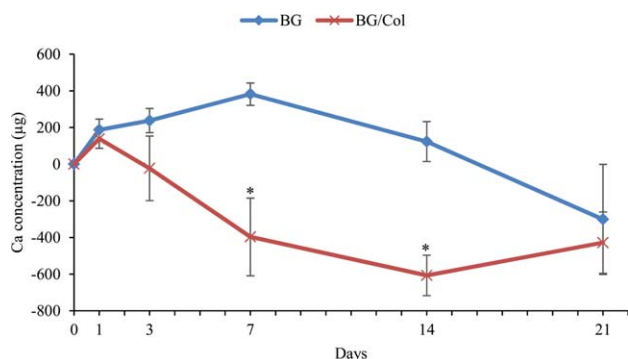


FIGURE 8. Cumulative calcium concentration in SBF for BG and BG/Col samples for up to 21 days. *BG/Col compared to BG; $p < 0.0001$.

expression evaluation). It was hypothesized that combination of inorganic material (represented by BG) and organic part (represented by Col) would constitute an improved scaffold, with similar natural bone characteristics and a suitable support to bone growth. SEM and EDX main findings demonstrated that Col could be successfully introduced into BG. Furthermore, a decrease in mass was observed over time for BG/Col, followed by a pH increase up to 9. On the other hand, BG samples presented no variation of mass,

with higher pH up to 11. Moreover, Ca assay demonstrated higher calcium uptake for BG/Col samples compared to BG during experimental periods, reaching same values 21 days postincubation. In addition, BG samples presented HA crystals formation on its surface after 14 days and, signs of initial degradation were observed for both materials (BG and BG/Col) after 21 days in SBF solution. BG and BG/Col FTIR spectra, showed defined peaks for HA formation after SBF incubation. Finally, a significant increase of BMSCs viability for both composites was observed compared to CG. qRT-PCR analysis indicated a decreased ALP gene expression for this cell type in the presence of BG/Col samples only in the first time point.

An ideal scaffold for bone tissue engineering should have interconnected porous structure, good biocompatibility and a composition well-matched with natural bones.^{30,31} An effective solution to reach this aim is to combine materials with organic and inorganic constitution. Our BG/Col composites were simple to manipulate and showed cohesion after PBS incubation. Furthermore, scaffold composition (80 and 20 wt % of BG and Col, respectively) was bio-inspired and aimed at mimicking natural bone composition and structure.³²⁻³⁴ This inorganic/organic proportion was obtained by impregnating BG scaffolds with Col solution which was

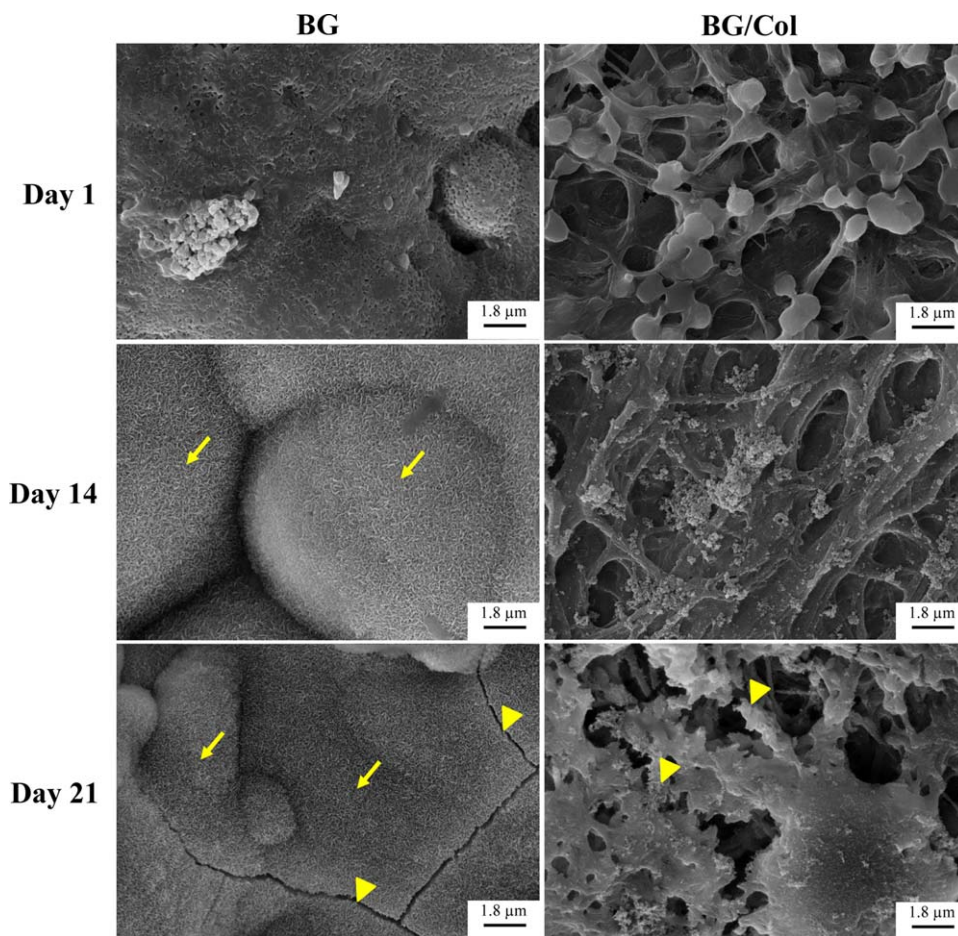


FIGURE 9. SEM representative micrographs of BG and BG/Col scaffolds after 1, 14, and 21 days of SBF incubation. Thin arrows indicate HA crystals; arrow heads indicate signs of degradation. Magnification of $\times 20,000$.

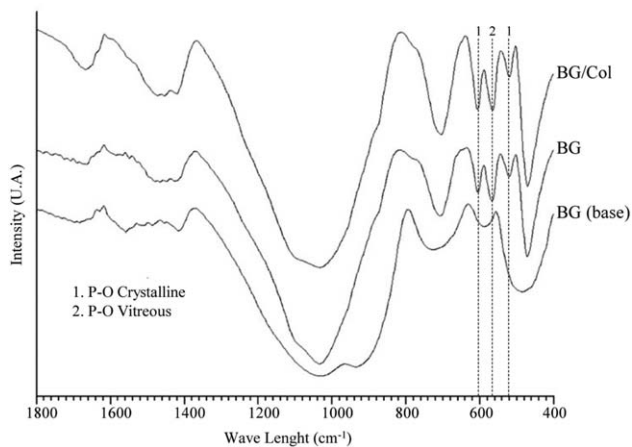


FIGURE 10. FTIR spectra for BG powder with no incubation (base), and BG and BG/Col scaffolds after 14 days of immersion in SBF. Arrows indicate HA peaks.

produced using the 0.5 g Col/100 mL AcOH ratio. This ratio was defined through several tests toward high amount of Col and low volume of AcOH to be used until the complete Col dissolution.

SEM micrographs after material preparation demonstrated that (i) Col was successfully impregnated all over the BG scaffold surface and (ii) this organic component was incorporated into the BG samples. Accordingly, EDX analysis indicated higher presence of C—one of the main components of Col³⁵—on the BG/Col scaffolds compared to BG, evidencing the Col on material surface. Additionally, EDX showed lower presence of Na and Si (BG chemical components)³⁶ on BG/Col surface compared to BG, demonstrating the effective Col coating/impregnation on BG scaffolds. Vacuum-based system, adapted from Camilo et al.,²¹ was used for an efficient Col impregnation of BG scaffolds (surface and pores). This is a fast and nonexpensive system that could be extensively used in biomaterials field²¹ to impregnate/coat different materials, utilizing diverse impregnation/coating solutions (organic or inorganic).

Also, it is worthwhile to highlight high porosity of BG scaffolds (around 80%), being this fact a key role to provide enough space to cell ingrowth and transport of nutrients, oxygen and growth factors.³⁷ On the other hand, it is known that a high porosity may imply in relatively low mechanical properties.³⁸ Still, highly porous BG/Col scaffolds may be suitable for filling and reconstructions in nonload-bearing areas.³⁸

Mass loss measurements showed that BG presented a constant sample mass during experimental periods and introduction of Col resulted in a decrease (especially after 1 day) of around 24% of the initial mass. It is known that rate of BG degradation is low which explain the constance of BG sample mass.³⁹

BG/Col scaffolds rise degradation may be associated to degradation of Col, since this organic component has rapid degradation rate.^{40–42} Col superior degradability may facilitate cell adhesion, proliferation and differentiation.⁴² Moreover, material degradation and liberation of space are indeed for subsequent substitution with neofomed bone and these points may improve performance of graft.^{43,44}

Values of pH measured in BG samples (around 11 in last experimental period) corroborate previous studies demonstrating that BG ion dissolution starts immediately after contact to fluids and produces an alkalization of immersion medium.⁴⁵ Interestingly, samples containing Col presented lower pH compared to BG samples (around 9). This phenomenon may be explained by protective effect of Col coating on BG surface, reducing bioactive material surface area, which may prevents abrupt alkalization of immersion medium.⁴⁶ Similarly, previous studies showed that incorporation of Col in Calcium phosphate and BG-based materials produced a more balanced pH, with values close to the physiological one.^{46,47} This behavior may create an appropriate microenvironment for cell growth and bone formation.⁴⁵

Furthermore, interaction between BG and SBF solution produced a Ca release and conversely Ca uptake observed on samples with Col. Ca release of BG corroborates well known material behavior when in contact to ion dissolution fluids.⁴⁸ Composite interface reactions are probable responsible for these behavior, releasing cations (Si, Na, Ca and P).²⁶ Differently, the Ca uptake of BG/Col samples may be related to the ability to mediate mineralization which is intrinsic to type I collagen fibers.⁴⁹ Ca uptake may contribute to HA-like layer formation on material surface, inducing biomaterial-tissue bonding and new bone formation.⁵⁰

SEM showed that HA layer was formed on BG surface after 14 days of SBF incubation, and this event is well-known for this kind of material.^{45,51} Although this layer was not evident on BG/Col, most probably due to collagen coating, BG and BG/Col FTIR indicated characteristics peaks for HA formation around 600 cm⁻¹,⁵¹ indicating mineralization for both materials.

Cell culture studies indicated higher cell viability for BG and BG/Col compared to CG, highlighting positive effect of BG and Col on cell metabolism and biocompatibility. This fact may be explained by the ion dissolution which happens immediately after the contact of bioactive glass with fluids^{45,52} and it is responsible by the stimulation of cell growth and proliferation.⁵³ According to previous studies, stimulatory effect of BG on osteoblast proliferation may be

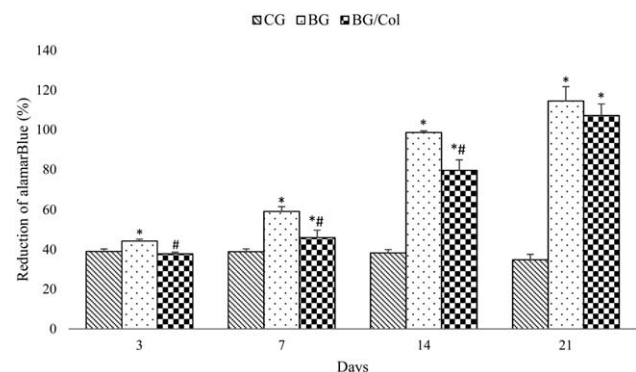


FIGURE 11. Cell viability by alamarBlue for BG and BG/Col scaffolds after different experimental periods of MSCs culture. *BG and BG/Col compared to CG at days 3 ($p < 0.01$ for BG), 7 ($p < 0.001$ and 0.05), 14 ($p < 0.001$) and 21 ($p < 0.001$); # BG/Col compared to BG at days 3 ($p < 0.001$), 7 ($p < 0.01$), 14 ($p < 0.001$).

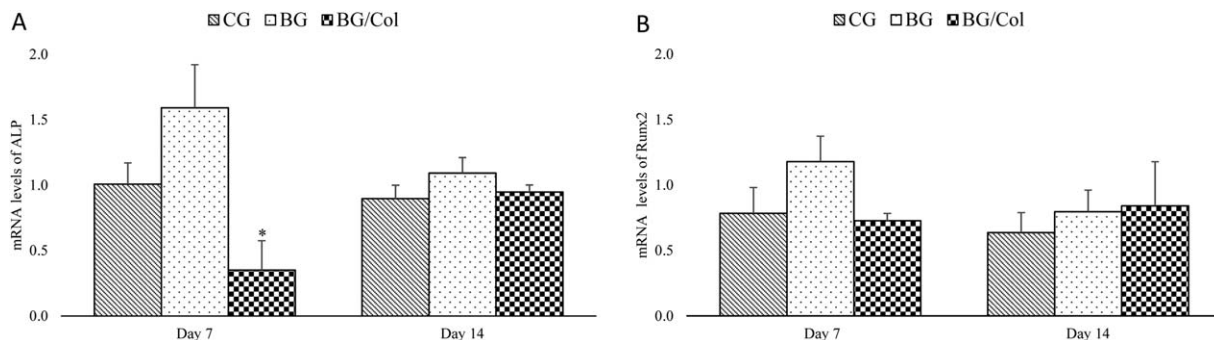


FIGURE 12. Relative expression levels of and ALP (A) Runx2 (B) for BG and BG/Col after 7 and 14 days of incubation with BMSCs. *BG compared to BG/Col ($p < 0.05$).

associated to insulin-like growth factor II (IGF-II).⁵⁴ Significant differences were found for cell viability comparing BG to BG/Col at days 3, 7, and 14. Interestingly, after last experimental period (21 days) no significant difference was observed between BG and BG/Col, equating both cell viabilities. One possible explanation for this event is that collagen coating degraded, expose BG bioactive surface and induce cell viability.⁵³ Although it was not observed stimulatory effect of the Col on cell viability, previous studies demonstrated that this organic component promoted cell attraction and proliferation *in vivo* toward new bone formation.⁵⁵ Therefore, further animal investigations are indeed in order to confirm high potential of vacuumed Col-impregnated BG scaffolds.

Data from qRT-PCR demonstrated decreased ALP gene expression for BMSCs in the presence of BG/Col samples only in the first time point (day 7). Probably, Col coating on the BG surface downregulated initial ALP gene expression of this bioactive material. Nevertheless, no difference was found after 14 days. Contrasting to that, some authors have demonstrated that BG and Col are capable of modulating the expression of ALP at different times.^{56,57} Similarly, no statistical difference of Runx2 was found when comparing to BG, BG/Col and CG at all periods. It is well-known that Runx2 is essential to commitment of early mesenchymal cells to osteoblast lineage and differentiation of osteoblasts.⁵⁸ We suggest, since cell proliferation and differentiation showed an inverse relationship,^{59,60} that cells were still at proliferation stage, as accessed by alamarBlue assay, and afterward they would progress to differentiation, expressing increased levels of ALP and Runx-2. Thus, further molecular studies with other experimental periods are necessary to elucidate bone-related gene expressions of BMSCs in contact with BG/Col composites.

Taken together, our research on novel BG and BG/Col composites are encouraging and conduct to additional molecular and cell culture investigations, and *in vivo* studies toward elucidation of bone-forming performance for tissue engineering applications.

CONCLUSIONS

This present study on BG scaffolds impregnated with Col showed that these composites could be produced by a low cost and efficient vacuum-based system. BG/Col scaffolds exhibited improved degradation, balanced pH upon PBS

incubation and mineralized Ca over time, accompanied by HA formation. Moreover, both BG and BG/Col scaffolds were biocompatible and noncytotoxic, promoting a higher cell viability compared to control. Future investigations should focus on additional molecular and *in vivo* studies in order to evaluate biomaterial performance for bone tissue engineering applications.

ACKNOWLEDGEMENT

H.W. Kido acknowledges Dr. J. Daguano from Multi users Central Facilities of UFABC for the SEM analysis.

REFERENCES

- Sarker B, Hum J, Nazhat SN, Boccaccini AR. Combining collagen and bioactive glasses for bone tissue engineering: A review. *Adv Healthc Mater* 2015;4(2):176–194.
- Jones JR. Review of bioactive glass: From Hench to hybrids. *Acta Biomater* 2013;9(1):4457–4486.
- Hench LL, David G. Interactions between bioactive glass and collagen: A review and new perspectives. *J Aust Ceram Soc* 2013; 49(2):1–40.
- Krishnan V, Lakshmi T. Bioglass: A novel biocompatible innovation. *J Adv Pharm Technol Res* 2013;4(2):78–83.
- Chen QZ, Ahmed I, Knowles JC, Nazhat SN, Boccaccini AR, Rezwan K. Collagen release kinetics of surface functionalized 45S5 Bioglass®-based porous scaffolds. *J Biomed Mater Res A* 2008;86(4):987–995.
- Deshmukh S, Dive A, Moharil R, Munde P. Enigmatic insight into collagen. *J Oral Maxillofac Pathol* 2016;20(2):276–283.
- Lee CH, Singla A, Lee Y. Biomedical applications of collagen. *Int J Pharm* 2001;221(1–2):1–22.
- Khan R, Khan MH. Use of collagen as a biomaterial: An update. *J Indian Soc Periodontol* 2013;17(4):539–542.
- Nijsure MP, Pastakia M, Spano J, Fenn MB, Kishore V. Bioglass incorporation improves mechanical properties and enhances cell-mediated mineralization on electrochemically aligned collagen threads. *J Biomed Mater Res A* 2017;105(9):2429–2440.
- Sharifi E, Ebrahimi-Barough S, Panahi M, Azami M, Ai A, Barabadi Z, Kajbafzadeh AM, Ai J. In vitro evaluation of human endometrial stem cell-derived osteoblast-like cells' behavior on gelatin/collagen/bioglass nanofibers' scaffolds. *J Biomed Mater Res A* 2016;104(9):2210–2219.
- Marelli B, Ghezzi CE, Barralet JE, Boccaccini AR, Nazhat SN. Three-dimensional mineralization of dense nanofibrillar collagen-bioglass hybrid scaffolds. *Biomacromolecules* 2010;11(6):1470–1479.
- Miri AK, Muja N, Kamranpour NO, Lepry WC, Boccaccini AR, Clarke SA, Nazhat SN. Ectopic bone formation in rapidly fabricated acellular injectable dense collagen-Bioglass hybrid scaffolds via gel aspiration-ejection. *Biomaterials* 2016;85:128–141.

13. Cancedda R, Dozin B, Giannoni P, Quarto R. Tissue engineering and cell therapy of cartilage and bone. *Matrix Biol* 2003;22(1):81–91.
14. Mastrogiacomo M, Scaglione S, Martinetti R, Dolcini L, Beltrame F, Cancedda R, Quarto R. Role of scaffold internal structure on in vivo bone formation in macroporous calcium phosphate bioceramics. *Biomaterials* 2006;27(17):3230–3237.
15. Stevens MM. Biomaterials for bone tissue engineering. *Mater Today* 2008;11(5):18–25.
16. Uejima S, Okada K, Kagami H, Taguchi A, Ueda M. Bone marrow stromal cell therapy improves femoral bone mineral density and mechanical strength in ovariectomized rats. *Cytotherapy* 2008;10(5):479–489.
17. Hernandez-Hurtado AA, Borrego-Soto G, Marino-Martinez IA, Lara-Arias J, Romero-Diaz VJ, Abrego-Guerra A, Vilchez-Cavazos JF, Elizondo-Riojas G, Martinez-Rodriguez HG, Espinoza-Juarez MA, Lopez-Romero GC, Robles-Zamora A, Mendoza Lemus OF, Ortiz-Lopez R, Rojas-Martinez A. Implant composed of demineralized bone and mesenchymal stem cells genetically modified with AdBMP2/AdBMP7 for the regeneration of bone fractures in ovis aries. *Stem Cells Int* 2016;2016:7403890.
18. Hussain S, Tamizhselvi R, George L, Manickam V. Assessment of the role of noni (*Morinda citrifolia*) juice for inducing osteoblast differentiation in isolated rat bone marrow derived mesenchymal stem cells. *Int J Stem Cells* 2016;9(2):221–229.
19. Hum J, Luczynski KW, Nooeaid P, Newby P, Lahayne O, Hellmich C, Boccaccini AR. Stiffness improvement of 45S5 bioglass (R)-based scaffolds through natural and synthetic biopolymer coatings: An ultrasonic study. *Strain* 2013;49(5):431–439.
20. Lee MH, You C, Kim KH. Combined effect of a microporous layer and type I collagen coating on a biphasic calcium phosphate scaffold for bone tissue engineering. *Materials* 2015;8(3):1150–1161.
21. Camilo CC, Silveira CAE, Faeda RS, de Almeida Rollo JMD, Purquerio BdM, Fortulan CA. Bone response to porous alumina implants coated with bioactive materials, observed using different characterization techniques. *J Appl Biomater Funct Mater* 2017;15(3):e223–e235.
22. Kido HW, Tim CR, Bossini PS, Parizotto NA, de Castro CA, Crovace MC, Rodrigues ACM, Zanotto ED, Filho OP, de Freitas Anibal F, Rennó ACM. Porous bioactive scaffolds: characterization and biological performance in a model of tibial bone defect in rats. *J Mater Sci Mater Med* 2015;26(2):74.
23. Yun H-S, Kim S-H, Khang D, Choi J, Kim H-H, Kang M. Biomimetic component coating on 3D scaffolds using high bioactivity of mesoporous bioactive ceramics. *Int J Nanomed* 2011;6:2521–2531.
24. Zorzi AR, Amstalden EMI, Plepis AMG, Martins VCA, Ferretti M, Antonioli E, Duarte ASS, Luzo ACM, Miranda JB. Effect of human adipose tissue mesenchymal stem cells on the regeneration of ovine articular cartilage. *Int J Mol Sci* 2015;16(11):26813–26831.
25. Kokubo T, Takadama H. How useful is SBF in predicting in vivo bone bioactivity? *Biomaterials* 2006;27(15):2907–2915.
26. Gabbai-Armelin PR, Cardoso DA, Zanotto ED, Peitl O, Leeuwenburgh SCG, Jansen JA, Renno ACM, van den Beucken JJJP. Injectable composites based on biosilicate® and alginate: handling and in vitro characterization. *RSC Adv* 2014;4(86):45778–45785.
27. van den Dolder J, Bancroft GN, Sikavitsas VI, Spauwen PHM, Jansen JA, Mikos AG. Flow perfusion culture of marrow stromal osteoblasts in titanium fiber mesh. *J Biomed Mater Res A* 2003;64A(2):235–241.
28. Zhang L, Chan C. Isolation and enrichment of rat mesenchymal stem cells (MSCs) and separation of single-colony derived MSCs. *J Vis Exp* 2010;(37):e1852.
29. Livak KJ, Schmittgen TD. Analysis of relative gene expression data using real-time quantitative PCR and the 2⁻ $\Delta\Delta$ CT method. *Methods* 2001;25(4):402–408.
30. Bose S, Roy M, Bandyopadhyay A. Recent advances in bone tissue engineering scaffolds. *Trends Biotechnol* 2012;30(10):546–554.
31. Amini AR, Laurencin CT, Nukavarapu SP. Bone tissue engineering: recent advances and challenges. *Crit Rev Biomed Eng* 2012;40(5):363–408.
32. Araújo GM, Vieites FM, Barbosa AA, Caramori Junior JG, Santos AL, Moraes GHK, Abreu JG, Muller ES. Variação aniônica da dieta sobre características ósseas de frangos de corte: Resistência à quebra, composição orgânica e mineral. *Arq Bras Med Vet Zootec* 2011;63:954–961.
33. Lopa S, Madry H. Bioinspired scaffolds for osteochondral regeneration. *Tissue Eng Part A* 2014;20(15–16):2052–2076.
34. Rother S, Salbach-Hirsch J, Moeller S, Seemann T, Schnabelrauch M, Hofbauer LC, Hintze V, Scharnweber D. Bioinspired collagen/glycosaminoglycan-based cellular microenvironments for tuning osteoclastogenesis. *ACS Appl Mater Interfaces* 2015;7(42):23787–23797.
35. Shoulders MD, Raines RT. Collagen structure and stability. *Annu Rev Biochem* 2009;78:929–958.
36. Hench LL, Xynos ID, Polak JM. Bioactive glasses for in situ tissue regeneration. *J Biomater Sci Polym Ed* 2004;15(4):543–562.
37. Long T, Yang J, Shi S-S, Guo Y-P, Ke Q-F, Zhu Z-A. Fabrication of three-dimensional porous scaffold based on collagen fiber and bioglass for bone tissue engineering. *J Biomed Mater Res B* 2015;103(7):1455–1464.
38. Hannink G, Arts JJC. Bioresorbability, porosity and mechanical strength of bone substitutes: What is optimal for bone regeneration? *Injury* 2011;42:S22–S25.
39. Sriranganathan D, Kanwal N, Hing KA, Hill RG. Strontium substituted bioactive glasses for tissue engineered scaffolds: the importance of octacalcium phosphate. *J Mater Sci Mater Med* 2016;27:39.
40. Mano JF, Silva GA, Azevedo HS, Malafaya PB, Sousa RA, Silva SS, Boesel LF, Oliveira JM, Santos TC, Marques AP, Neves NM, Reis RL. Natural origin biodegradable systems in tissue engineering and regenerative medicine: Present status and some moving trends. *J R Soc Interface* 2007;4(17):999–1030.
41. Cao Y, Wang B. Biodegradation of silk biomaterials. *Int J Mol Sci* 2009;10(4):1514–1524.
42. Wu Y, Wong YS, Fuh JYH. Degradation behaviors of geometric cues and mechanical properties in a 3D scaffold for tendon repair. *J Biomed Mater Res Part A* 2017;105(4):1138–1149.
43. Gu Y, Chen L, Yang H-L, Luo Z-P, Tang T-S. Evaluation of an injectable silk fibroin enhanced calcium phosphate cement loaded with human recombinant bone morphogenetic protein-2 in ovine lumbar interbody fusion. *J Biomed Mater Res Part A* 2011;97A(2):177–185.
44. van de Watering FCJ, van den Beucken JJJP, Walboomers XF, Jansen JA. Calcium phosphate/poly(d,l-lactic-co-glycolic acid) composite bone substitute materials: evaluation of temporal degradation and bone ingrowth in a rat critical-sized cranial defect. *Clin Oral Implants Res* 2012;23(2):151–159.
45. Rahaman MN, Day DE, Sonny Bal B, Fu Q, Jung SB, Bonewald LF, Tomsia AP. Bioactive glass in tissue engineering. *Acta Biomater* 2011;7(6):2355–2373.
46. Ueno FR, Kido HW, Granito RN, Gabbai-Armelin PR, Magri AM, Fernandes KR, da Silva AC, Braga FJ, Renno AC. Calcium phosphate fibers coated with collagen: In vivo evaluation of the effects on bone repair. *Biomater Eng* 2016;27(2–3):259–273.
47. Magri AMP, Fernandes KR, Ueno FR, Kido HW, da Silva AC, Braga FJ, Granito RN, Gabbai-Armelin PR, Rennó ACM. Osteoconductive properties of two different bioactive glass forms (powder and fiber) combined with collagen. *Appl Surf Sci* 2017;423:557–565.
48. Hench LL. *Introduction to Bioceramics*, 2nd ed. London: Imperial College Press; 2013. p 620.
49. Nudelman F, Pieterse K, George A, Bomans PHH, Friedrich H, Brylka LJ, Hilbers PAJ, de With G, Sommerdijk NAJM. The role of collagen in bone apatite formation in the presence of hydroxyapatite nucleation inhibitors. *Nat Mater* 2010;9(12):1004–1009.
50. Chang K-C, Chang C-C, Chen W-T, Hsu C-K, Lin F-H, Lin C-P. Development of calcium phosphate/sulfate biphasic cement for vital pulp therapy. *Dent Mater* 2014;30(12):e362–e370.
51. Łączka M, Cholewa-Kowalska K, Osyczka AM. Bioactivity and osteoinductivity of glasses and glassceramics and their material determinants. *Ceram Int* 2016;42(13):14313–14325.
52. Hoppe A, Güldal NS, Boccaccini AR. A review of the biological response to ionic dissolution products from bioactive glasses and glass-ceramics. *Biomaterials* 2011;32(11):2757–2774.
53. Tsigkou O, Jones JR, Polak JM, Stevens MM. Differentiation of fetal osteoblasts and formation of mineralized bone nodules by

- 45S5 Bioglass[®] conditioned medium in the absence of osteogenic supplements. *Biomaterials* 2009;30(21):3542–3550.
54. Xynos ID, Edgar AJ, Buttery LDK, Hench LL, Polak JM. Ionic products of bioactive glass dissolution increase proliferation of human osteoblasts and induce insulin-like growth factor II mRNA expression and protein synthesis. *Biochem Biophys Res Commun* 2000; 276(2):461–465.
 55. Fu-Yin H, Meng-Ru L, Ru-Chun W, Hsiu-Mei L. Hierarchically biomimetic scaffold of a collagen–mesoporous bioactive glass nanofiber composite for bone tissue engineering. *Biomed Mater* 2015; 10(2):025007.
 56. Zahid S, Shah AT, Jamal A, Chaudhry AA, Khan AS, Khan AF, Muhammad N, ur Rehman I, lu R. Biological behavior of bioactive glasses and their composites. *RSC Adv* 2016;6(74):70197–70214.
 57. Viale-Bouroncle S, Gosau M, Morsczeck C. Collagen I induces the expression of alkaline phosphatase and osteopontin via independent activations of FAK and ERK signalling pathways. *Arch Oral Biol* 2014;59(12):1249–1255.
 58. Huang W, Yang S, Shao J, Li Y-P. Signaling and transcriptional regulation in osteoblast commitment and differentiation. *Front Biosci* 2007;12:3068–3092.
 59. Shang Z-Z, Li X, Sun H-Q, Xiao G-N, Wang C-W, Gong Q. Differentially expressed genes and signalling pathways are involved in mouse osteoblast-like MC3T3-E1 cells exposed to 17- β estradiol. *Int J Oral Sci* 2014;6(3):142–149.
 60. Ruijtenberg S, van den Heuvel S. Coordinating cell proliferation and differentiation: Antagonism between cell cycle regulators and cell type-specific gene expression. *Cell Cycle* 2016;15(2):196–212.